8-19-2024

Erodibility of Sand-Silt-Xanthan Gum Mixtures

Edwin Kotey
University of South Carolina

Erodibility of Sand-Silt-Xanthan gum Mixtures

by

Edwin Dzanie Kotey

Bachelor of Science
Kwame Nkrumah University of Science and Technology, 2016

Submitted in Partial Fulfillment of the Requirements

For the Degree of Master of Science in

Civil Engineering

College of Engineering and Computing

University of South Carolina

2024

Accepted by:

Enrica Viparelli, Director of Thesis

Hanif Chaudhry, Reader

Jasim Imran, Reader

Ann Vail, Dean of the Graduate School

Acknowledgements

Many thanks to post-doctoral researcher Matthew Czapiga for being a great help and guide and the many undergraduate researchers who helped with experimental setup and construction, Frankie DiCrocco, Brandon Lopez, Megan Smith, Jonathan Hughes, Oru-Ntui Nkiri, Lylie Wilkie, and Anne Lazureanu. This research was funded by the U.S Army Engineer Research and Development Center.

Abstract

The high frequency of earthen embankment failure recorded during floods has led to the general rule that embankments should not be overtopped. This notwithstanding, overtopping cannot be entirely avoided particularly during extreme events, such as winter storms and hurricanes. Reducing soil erodibility is thus fundamental to prevent and control disasters caused by embankment failure. Recent studies have explored the use of environmentally friendly additives, such as biopolymers, to improve soil properties. Geotechnical tests have shown that biopolymers can effectively increase soil strength, but little is known about biopolymer-treated soil resistance to erosion by flowing water. Results of flume experiments to characterize erosion of biopolymer-treated sand-silt mixtures are presented here. Experiments were conducted in the Hydraulics Laboratory at the University of South Carolina with xanthan gum as biopolymer additive. Proctor tests were first performed to identify the optimum water content of different sand-silt-xanthan gum mixtures differing in silt and xanthan gum content. Findings show a positive correlation between xanthan gum concentration and optimum water content of sand. In sand-silt mixtures, on the contrary, optimum water content does not appreciably vary with xanthan gum content. The erodibility of mixtures of sand, silt and xanthan gum was measured in a laboratory flume for increasing values of the boundary shear stress. To meaningfully compare results, the water content of the samples was always equal to the optimum value. Erodibility tests indicated that erodibility of xanthan gum-treated sands decreased with increasing xanthan gum concentration. Further, the mode of sediment entrainment in transport changed from grain-grain detachment at low xanthan gum concentrations, to plucking at comparatively high biopolymer contents. The same transition from grain-grain erosion to plucking was observed at relatively low xanthan gum contents for increasing bed shear stress. Characterizing the erodibility of sand-silt-xanthan gum mixtures was challenging due to the high mobility of silt size particles. In general, sand-silt-xanthan gum mixtures were harder to erode than sand-xanthan gum mixtures with the same biopolymer content. The difference between erodibility of xanthan gum-treated sand and treated sand-silt mixtures increased with biopolymer and silt content. In addition, at low xanthan gum concentration, silt was entrained in suspension and erosion of the remaining sand-xanthan gum mixture occurred as observed in absence of silt, that is grain-grain erosion at low boundary stress and plucking at high boundary stress. For increasing xanthan gum content, silt became hard to entrain in suspension, and the erosion mode transitioned from entrainment of sand grains to plucking.

Table of Contents

List of Tables

List of Figures

Chapter 1: Introduction

Dams and embankments have been built for a very long time. The Egyptians are known to have constructed the first dam about 5,000 years ago and the Romans are known to have constructed the first concrete dam some 2,000 years ago (Yang; et al., 1999).

Even though construction of dams, and for that matter earthen embankments, started many centuries ago, cases of embankment failures have occurred throughout history. However, it was not until events in 1972, The Buffalo Creek incident, (Sharma & Kumar, 2013), 1976, Teton Dam failure, (Bolton Seed & Duncan, 1987), and 1977, Kelly Barnes Dam failure, that the US government started to establish dam safety programs (DeNeale et al., 2019)

In 1975, a US Committee on large dams stated that about 80% of large dams in the country were made from erodible materials (Wu, 2011). In 1985 earthen embankments constitute more than 93% of the total number of dams in the US (Costa, 1985).

Out of the over 91,000 dams in the US with an average life span of 63 years, about 76% are classified as High Hazard Potential Dams, that is over 69,100 dams (USACE, 2024). Not long ago, the ASCE/EWRI Task Committee on Dam/Levee Breaching raised the concern that most earthen embankments may likely fail under extreme conditions (Wu, 2011).

In October 2015 Hurricane Joaquin produced excessive rainfall that caused extensive damage in the state of South Carolina. The heavy rainfall which continued for 5 days (October 1 – 5) was deemed a 1000-year rainstorm event as the amount of rainfall recorded in a 48hour period was 35.81cm although some areas also recorded more than 50 cm in 24-hour duration (Tabrizi et al., 2017).

The total number of dams that was reported as breached by the South Carolina Department of Health and Environmental Control (SC-DHEC) was 47 with 22 dams being located within the Columbia Area (Sasanakul et al., 2017).

In general, main causes of embankment failure are overtopping, foundation and structural defects, and piping (Sharma & Kumar, 2013) with overtopping accounting for more than one-third of all dam failures (Costa, 1985). This reason has led to the general rule that embankments must not be overtopped as erosion due to overtopping is the leading cause of embankment failure (George R. Powledge; et al., 1989). It is therefore possible that if the resistance to erosion of such embankments is improved, failures of dams will be lessened.

Currently employed erosion protection techniques include the use of geotextiles, grass vegetation, concrete blocks, cement-modified soils, riprap, and gabions (George R. Powledge; et al., 1989). These techniques present serious drawbacks when applied in the real world. For example, the use of cement is not environmentally friendly due to greenhouse gas emissions, and chemical additives have been proven to have different levels of toxicity (Ko & Kang, 2018). Recent studies show that environmentally friendly soil additives such as biopolymers have the potential of reducing soil erodibility with limited adverse effects (Abdelaziz et al., 2019; Chang et al., 2015; Ko & Kang, 2018).

The research presented in this thesis sheds light on how the inclusion of biopolymers, specifically xanthan gum, in sand and sand-silt mixtures increases resistance to erosion by flowing water. The main reasons of choice for xanthan gum are its commercial availability and well adopted industrial and agricultural use (Abdelaziz et al., 2019).

Results of laboratory experiments performed in the Hydraulics Laboratory at the University of South Carolina are reported. These experiments investigated how erodibility of a mixture of sand, silt, xanthan gum and water vary with biopolymer and silt content. A mixture of sand-sized particles with geometric mean size equal to 0.42 mm and geometric standard deviation equal to 1.81 was mixed with xanthan gum in the baseline experiments. Silica flour (silt-size sediment) was then added to the sand at 10% and 25% mass concentrations. The soil-xanthan gum mixtures were obtained by adding 0.05 – 0.5% xanthan gum by mass relative to the non-cohesive sediment. To compare results of different tests, all mixtures were obtained using a volume of water equal to the optimum water content.

This thesis is organized as follows. Background information on biopolymers is first presented. An overview of the laboratory experiments and a description of experimental procedures is presented in section three. Experimental results are summarized in section four with proctor test results followed by results of erodibility tests. Proctor tests (ASTM, 2021) were performed to determine if and how the use of xanthan gum, as an additive to mixtures of non-cohesive soil, impacts the optimum water content, that is a critical property for the design of embankment material and to reduce soil erodibility. In the erodibility tests soil samples were placed at the bottom of a laboratory flume and erosion rates were measured for different values of flow velocity (boundary shear stress).

Chapter 2: Biopolymers and Erosion

2.1 Characteristics of biopolymers relevant to this study:

Biopolymers are produced by naturally occurring biological processes and are made up of many small monomeric units (Cho & Chang, 2018). Three main types of biopolymers are commonly identified: polynucleotides, that is RNA and DNA, polypeptides from amino acids, and polysaccharides (cellulose and chitosan) (Cho & Chang, 2018). Examples of biopolymers considered for geotechnical applications include gellan gum, chitosan, curdlan, xanthan gum, agar gum, and scleroglucan (Chang et al., 2016).

When mixed with natural soils, biopolymers increase the soil liquid limit by increasing viscosity of pore fluid and soil wettability through water adsorption (Chang et al., 2020). As a result, hydrogels form in the pores, surround the grains, and reduce soil hydraulic conductivity (Chang et al., 2016). Biopolymer-treated sands have higher soil strength than natural sand due to the matrix formed by biopolymers and fine soil particles (Abdelaziz et al., 2019; Chang et al., 2015; Cho & Chang, 2018).

In the experiments presented below, xanthan gum was used for its commercial availability and numerous applications in the field and in the laboratory (Abdelaziz et al., 2019; Chang et al., 2015, 2016). Xanthan gum is a polysaccharide derived from the bacterium Xanthomonas campestris through the fermentation of glucose or sucrose (Cho & Chang, 2018).

2.2 Erosion Mechanisms:

Erosion is the gradual removal of sediment from a surface. Understanding the factors that allow for sediment transport and erosion is crucial to characterize soil behavior in the presence of flowing water. In general, erosion rates vary with flow velocity and sediment composition. The typical mode of erosion of loose alluvium is characterized by the flow entraining individual grains in transport. In case of soils that are harder to erode, however, erosion is broadly classified into abrasion by moving particles, plucking or removal of broken pieces from the bed, and macroabrasion that consists of moving particles fracturing the soil surface into pieces that can be removed by plucking (Chatanantavet & Parker, 2009).

Erosion rates by flowing water are generally computed with empirical models as functions of the shear stress acting on the soil surface, soil properties and water properties. Common simplification of erosion models is the introduction of a reference (or critical) value of the shear stress below which sediment is not eroded. Experiments performed in 1970s, however, clearly show that while these thresholds can be useful for the formulation of empirical models, they do not have a well-defined physical meaning because if sediment is exposed to flowing water for long enough time, some particles will always move (Paintal, 1971; Parker, 2008).

There are different types of tests to measure erosion rates. The three main types are jet erosion test (JET), hole erosion test (HET), and flume-type erosion test (Clar & T., 2007).

JET involves directing a hydraulic jet towards an exposed soil surface and measuring the rate of erosion during the process. It is used in both laboratory and field situations and works best for cohesive soils. HET consists in studying erosion around a pre-drilled hole in the soil sample and is used to characterize piping erosion. Flume tests are used in determining erosion rates in presence of relatively large shear stresses such as those typical of stream bank erosion, spillway headcut erosion, and rill erosion amongst others (McNichol et al., 2017). In this study, flume erosion is employed to study soil erodibility in the context of a research project on breach development in earth embankments during overtopping.

Chapter 3: Methodology

3.1 Sediment size distribution:

The gradation of the sand-silt mixtures prepared and used in the experiments is shown in Figure B.1 and is similar to other grain size distributions used in previous studies on the use of xanthan gum as additive to improve mechanical properties of sand (Abdelaziz et al., 2019; Chang et al., 2015, 2016). The grain size distributions of Figure B.1 were measured with a combination of sieve analysis for sizes greater than 62.5 microns, and hydrometer test for particles in the silt range. The soil hydrometer used was the 151H (ASTM, 2021).

The blue line of Figure B.1 is the grain size distribution of the sand, with geometric mean size, D_g = 0.42 mm, median diameter D_{50} = 0.44 mm and geometric standard deviation s_g = 1.81. The yellow line represents the silt grain size distribution. Two sand-silt mixtures were used in the experiments and were obtained adding 10% and 20% by mass to the sand of Figure B.1 which are the gray and orange lines shown respectively. Central diameters of the sediment size distribution of the sand-silt mix with 10% silt content were D_g = 0.29 mm, D_{50} = 0.35 mm, and geometric standard deviation s_g = 3.32 mm. For the sand-silt mixture with 25% silt by mass D_g was 0.18 mm, D_{50} 0.27, and s_g 4.98

3.2 Rheology of Xanthan Gum:

The viscosity of water-xanthan gum mixtures was measured using a DV Next Rheometer. These measurements were performed to compare the behavior of the materials used in the experiments at the University of South Carolina with those performed in previous experiments (Casas & García-Ochoa, 1999; Morris et al., 1977).

Viscosity, m, is a measure of internal friction of a fluid. It is defined as the ratio of shear stress to the shear rate of the material.

$$\mu = \frac{shear\ stress}{shear\ rate} = \frac{\tau}{\gamma}$$

Equation 1: Viscosity Equation

To further understand the rheology of xanthan gum, different solutions of the mixture were prepared and with the aid of the of the rheometer results different curves for different water content were produced.

A plot of shear rate (1/sec) against shear stress (Pa) was made as shown below in Figure B.2 to classify the rheology of the mixture. By using Equation 16a provided in (Imran et al., 2001), it was observed that the mixture changed from a Newtonian fluid for very low concentrations of xanthan gum (0.05%) to a Bingham model (bilinear rheology) for higher xanthan gum concentrations (1% and 2%). For bilinear rheology, it means at very low strain rates, the flow exhibits properties of a Newtonian fluid, with high viscosity (Imran et al., 2001). Also, it can be seen from the chart that higher yield strength and shear stress correspond with higher xanthan gum concentration.

$$\frac{\tau}{\tau_{ya} sgn(\gamma)} = 1 + \frac{|\gamma|}{\gamma_r} - \frac{1}{1 + r\frac{|\gamma|}{\gamma_r}}$$

Equation 2: Equation 16a from (Imran et al., 2001) where:

$$r = \frac{|\gamma|}{\gamma_r}; \qquad \gamma_r = \frac{\tau_{ya}}{\mu_h}$$

Equation 3: Equation 16b,c from (Imran et al., 2001)

Apparent and specific yield strengths are described by τ_{ya} and τ_y respectively. By fitting the results generated to the above equation, the lines of best fit were obtained. Fitting parameters were obtained by using *Solver* in Excel. Also, for Figures 2b and 2c, the values for stress were divided by 10 to allow for reasonable plotting of values and acquisition of fitting parameters.

3.3 Preparation of biopolymer-treated samples:

Sand, silt and xanthan gum are mixed with a water content equal to the optimum value to compare results of experiments conducted with different soil and shear stress. The optimum water content of each mixture was determined with a proctor test (ASTM reference). Samples were prepared using the wet mixing method as that has been found to be the best way of mixing biopolymers with sand as it allows for effective polymerization of the biopolymer powder while enhancing interactions between the biopolymer-filler and uniform water distribution(Abdelaziz et al., 2019).

This method consists in measuring the required water content for each mixture and gradually adding xanthan gum to the water. For each addition of xanthan gum into water, a hand drill was used to mix the solution for about 45 seconds. When all the xanthan gum is mixed with water, the solution was continually stirred with the hand drill until a relatively even and viscous gel-like mixture formed (Figure B.3a). This solution was then added to the sediment and stirred with a hand drill until the xanthan gum solution uniformly mixed with all the sand. (Figure B.3b).

For mixtures containing silt, a small portion of water was used to dampen the silt. This was done to prevent silt particles from floating into the air when being mixed with the sediment, as such occurrences are hazardous to the respiratory system. Once the silt was mixed with sand, the already prepared biopolymer gel mixture was added and mixed with a hand drill until a uniform mixture was achieved. Mixing silt and sand and before adding xanthan gum solution reduced the formation of large lumps of silt and biopolymer that would have represented weaknesses of the soil during the erodibility tests. In other words, these lumps would have been ideal candidates for plucking-type of erosion.

3.4 Optimum water content:

Proctor tests were initially conducted following the procedure outlined in the ASTM 698 for Standard Proctor Test (ASTM, 2021), i.e. 2% of water was periodically added to the same sample of xanthan gum-treated sediment. This procedure, however, did not produce consistent results (Figure B.4a) for the complex interaction between water, biopolymer, and sediment particles. Also, for ASTM 698 there must be clear rise and fall in the data points with optimum water content being the maximum. However, this was not the case in the many tests that were conducted. For this reason, the proctor test procedure was modified as follows: a new sediment-biopolymer sample was prepared for each step of the proctor test. This method provided repeatable estimates of optimal water content (Figure B.4b) and was thus preferred to the ASTM method (Figure B.4).

3.5 Experimental Setup:

A schematic drawing of the erodibility flume is presented in Figure B.5. The flume consisted of two modified 1.32 m^3 tote tanks connected end to end by a 4.9 m long suspended channel. The width of the channel was 26 cm. The sediment box which had a dimension of 22 cm x 22 cm was located 2.8 m from the flume entrance. The box was made of plexiglass and a vertically moving platform was attached to a cylindrical rod and connected to a jack. The jack was calibrated, and the platform elevation varied of 0.3 cm for each quatre (90 degree) turn, that is moving the knob from a 12-hour mark to the 3-hour mark on a clock. Sediment samples were placed on the platform and made flush with the flume bottom. As sediment was eroded, the platform was raised by a known amount.

Water was supplied from an overhead tank through a 6-inch line to the upstream tank. Discharge was measured with a manometer connected to an orifice plate. The inlet of water in the flume was controlled with a broad crested weir located 20 cm downstream of the flume entrance. A tail weir located at the downstream exit end of the downstream tank is used to control the downstream water level and to return water to the sump of the laboratory. Flow conditions in the erodibility tests were determined based on values of velocity, U, and boundary shear stress t_b. The shear velocity $u^* = \sqrt{\tau_b/\rho}$ then computed to express soil erodibility as function of soil and flow properties. Characteristics of the flow used in the experimental runs are presented in Table A.1 where Q denotes the flow discharge and y_s the water depth at the flume exit.

The preparation of the erodibility tests consisted in placing a compacted layer of highly concentrated (1% xanthan gum) biopolymer-treated sand on the movable platform in the sediment box. This layer prevented water from seeping through the sample. The soil sample was then placed on top of the highly concentrated sand and compacted to ensure it was not loosely packed which would have caused easy erosion of the sample.

The compacted sample was made flush to the surface of the channel and covered with plastic and a lid. This helped keep the sample intact when the flume was being filled with water prior to starting each run. After the flume was filled with water the lid and plastic were carefully removed and the sample was raised to a height equal to 0.3cm above the bed and the experiment started.

At the end of the experiment, the number of cranks, is then divided by the total time to attain the erosion rate:

$$erosion\ rate, \varepsilon = \frac{\text{number of cranks x 0.3}}{\text{total duration of experiment}}$$

Each run lasted for 30 minutes, as done with previous erosion tests (Chen, 2006).

Chapter 4: Results and Discussion

4.1 Proctor Test and Rheology:

The results for the proctor test are summarized Table A.2 and Figure B.6. For xanthan gum-treated sand, as the concentration of xanthan gum increases so does the optimum water content. However, for sand-silt mixtures the optimum water content remains relatively constant for increasing xanthan gum concentration.

Experimental results further suggest that at xanthan gum concentrations smaller than 0.2%, the optimum water content increases with silt content with maximum value that is reached (compared to orange and grey lines in Figure B.6) around 10% silt concentration. This was confirmed by performing further proctor tests at 0.05% xanthan gum concentration, as reported in Table A.3. For higher xanthan gum concentrations there was no variation in optimum water content with silt content.

Furthermore, the rheology of xanthan gum can be described as changing from linear to bilinear based on the concentration of xanthan gum in the solution. As very low concentrations do not significantly alter the make up of solution, it behaves almost the same as water. However, as the concentration of the xanthan gum in the solution is increased, a change is observed as shown in Figure B.2.

4.2 Erosion Tests:

Erosion test results are presented in Table A.4 for xanthan gum concentrations equal to 0.05%, 0.1 % and 0.15%. At higher concentration values of xanthan gum soil erodibility was too small to be measurable in the flume of Figure B.5.

Table A.4 clearly indicates that, for a given bed shear stress and silt content, erosion rate decreases as the biopolymer concentration increases. This is due to swelling of the xanthan gum in the pores of the sample which creates a matrix between individual grains.

Changes in erosion rate with shear stress for various concentrations of xanthan gum are illustrated in Figures 7a, 7b and 7c for different sand-silt contents (blue, orange and grey lines). As expected, erosion rate increases with bed shear stress for a given xanthan gum concentration. At 0.05% xanthan gum concentration (Figure B.7a), no difference is observed between the sand sample and the mixture with 10% silt content at relatively low bed shear stress. At such low xanthan gum concentration, erosion rate decreases for the mixture with 25% silt content. At higher xanthan gum concentrations (Figures 7b and 7c), erosion rate decreases with increasing silt content.

The lack of difference of erosion rate between the sand and the mixture with 10% silt content at 0.05% xanthan gum concentration and lower shear stress (runs 2 - 5) can be explained because of the paucity of xanthan gum concentration to create a matrix within silt particles. In other words, there is not a high enough content of silt and biopolymer to make a difference.

At bed shear stress greater than 9.3 Pa (runs 5 and 6), there is a sudden increase in erosion rate. This corresponds to a change in the mode of erosion, from grain-grain (typical of loose alluvium) and abrasion to plucking and macroabrasion with large lumps being plucked from the surface and transported downstream.

Furthermore, the relation between erosion rate and the bed shear stress for all the samples are shown below in Figure B.8. Chart for 0% Silt (Figure B.8a) indicates a power relation between bed shear stress and erosion rate for 0.05% xanthan gum whereas 0.1% xanthan gum and 0.15% xanthan gum show a linear relationship for the range of bed shear stress that was applied. Same can be observed with 25% silt (Figure B.8c) except for 0.15% xanthan gum which was characterized by one erosion point. For 10% silt (Figure B.8b), an exponential relation provided the best fit for both 0.05% and 0.1% xanthan gum mixtures.

As can be observed, the least erosion is recorded on the 25% silt chart, and the highest on the 10% silt chart as explained above.

It is worth noting that the shear stresses developed under these experimental conditions resulted in only two points for high samples that had xanthan gum and silt concentrations. For this reason, a line was used in fitting those points as we have only two points.

Chapter 5: Conclusion

Results of Proctor Tests performed on sand-silt-xanthan gum mixtures indicate that the optimum water content rises as the concentration of xanthan gum is increased in biopolymer treated sands. At low xanthan gum concentrations, the optimum water content increases with silt content until a maximum is reached and decreases from 10% to 25% silt content, as confirmed with 0.05% xanthan gum concentration additional tests.

Xanthan gum concentration, as well as silt content, does play a role in the erosion rate of sediments. Erodibility tests indicated that erodibility of xanthan gum-treated sands decreased with increasing xanthan gum concentration. Further, the mode of sediment entrainment in transport changed from grain-grain detachment at low xanthan gum concentrations, to plucking (lump removal) at comparatively high biopolymer contents. The same transition from grain-grain erosion to plucking was observed at relatively low xanthan gum contents for increasing bed shear stress.

Experiments on erodibility of sand-silt-xanthan gum mixtures showed that these mixtures were harder to erode than sand-xanthan gum mixtures with the same biopolymer content. The difference between erodibility of xanthan gum-treated sand and treated sand-silt mixtures increased with biopolymer and silt content.

At low xanthan gum concentration, silt was entrained in suspension and erosion of the remaining sand-xanthan gum mixture occurred as observed in absence of silt, that is grain-grain erosion at low boundary stress and lump erosion at high boundary stress. For increasing xanthan gum content, silt became hard to entrain in suspension, and the erosion mode transitioned from entrainment of sand grains to plucking. Further investigation is required to thoroughly characterize the erodibility of biopolymer treated sand-silt mixture and assess the applicability in the real world.

References

Abdelaziz, S., Gersappe, D., Rafailovich, D., Gersappe (co-Pi, D., & Rafailovich, M. (2019). *Biopolymer-Stabilized Earth Materials for Resilient and Adaptable Infrastructures*.

ASTM. (2021). *Standard Test Methods for Laboratory Compaction Characteristics of Soil Using Standard Effort*. *08*(Reapproved 1989), 3–4. https://doi.org/10.1520/D0698-12R21.

Bolton Seed, H., & Duncan, J. M. (1987). The failure of Teton Dam. *Engineering Geology*, *24*(1–4), 173–205. https://doi.org/10.1016/0013-7952(87)90060-3

Chang, I., Im, J., & Cho, G. C. (2016). Introduction of microbial biopolymers in soil treatment for future environmentally-friendly and sustainable geotechnical engineering. *Sustainability (Switzerland)*, *8*(3). https://doi.org/10.3390/su8030251

Chang, I., Im, J., Prasidhi, A. K., & Cho, G. C. (2015). Effects of Xanthan gum biopolymer on soil strengthening. *Construction and Building Materials*, *74*(January), 65–72. https://doi.org/10.1016/j.conbuildmat.2014.10.026

Chang, I., Lee, M., Tran, A. T. P., Lee, S., Kwon, Y. M., Im, J., & Cho, G. C. (2020). Review on biopolymer-based soil treatment (BPST) technology in geotechnical engineering practices. *Transportation Geotechnics*, *24*(June), 100385. https://doi.org/10.1016/j.trgeo.2020.100385

Chatanantavet, P., & Parker, G. (2009). Physically based modeling of bedrock incision by abrasion, plucking, and macroabrasion. *Journal of Geophysical Research: Earth Surface*, *114*(4), 1–22. https://doi.org/10.1029/2008JF001044

Chen, J.-L. B. H.-C. (2006). The EFA, Erosion Function Apparatus: An overview. *Proceedings of the 16th International Conference on Soil Mechanics and Geotechnical Engineering*, 479–481.https://doi.org/10.1016/0266-1144(84)90012-8

Cho, G., & Chang, I. (2018). *Cementless Soil Stabilizer – Biopolymer*.

Costa, J. E. (1985). Floods from Dam Failures . In *U.S. Geological Survey* (Vol. 2).

DeNeale, S. T., Baecher, G. B., Stewart, K. M., Smith, E. D., & Watson, D. B. (2019). *Current State-of-Practice in Dam Safety Risk Assessment* (Issue December).

George R. Powledge;, Ralston;, D. C., Miller;, P., Chen;, Y. H., Clopper;, P. E., & Temple, D. M. (1989). Mechanics of Overflow Erosion on Embankments. I: Research Activities. *Journal of Hydraulic Engineering*, *115*(8), 1040–1055.Imran, B. J., Member, A., Parker, G., Locat, J., & Lee, H. (2001). *1D NUMERICAL MODEL OF MUDDY SUBAQUEOUS AND SUBAERIAL DEBRIS FLOWS*. *127*(November), 959–968.

Ko, D., & Kang, J. (2018). Experimental studies on the stability assessment of a levee using reinforced soil based on a biopolymer. *Water (Switzerland)*, *10*(8). https://doi.org/10.3390/w10081059

McNichol, B., Kassa, K., Fox, G., Miller, R., & Guertault, L. (2017). Erodibility Parameters Derived from Jet and Flume Erosion Tests on Root-Permeated Soils. *Journal of Contemporary Water Research & Education*, *160*(1), 119–131. https://doi.org/10.1111/j.1936-704x.2017.03244.x

Paintal, A. S. (1971). Concept Of Critical Shear Stress In Loose Boundary Open Channels. *Journal of Hydraulic Research*, *9:1*, 91–113. https://doi.org/10.1080/00221687109500339

Parker, G. (2008). Transport of Gravel and Sediment Mixtures. *Sedimentation Engineering: Processes, Measurements, Modeling, and Practice*, *110*, 165–252. https://doi.org/10.1061/9780784408148.ch0

Sasanakul, I., Gassman, S. L., Pierce, C. E., Ovalle, W., Starcher, R., Gheibi, E., & Rahman, M. (2017). *Dam Failures from a 1000-Year Rainfall Event in South Carolina*. *March*, 244–254. https://doi.org/10.1061/9780784480458.024

Sharma, R. P., & Kumar, A. (2013). Case Histories of Earthen Dam Failures. *Seventh International Conference on Case Histories in Geotechnical Engineering*, *May*, 8.

Tabrizi, A. A., LaRocque, L. A., Chaudhry, M. H., Viparelli, E., & Imran, J. (2017). Embankment Failures during the Historic October 2015 Flood in South Carolina: Case Study. *Journal of Hydraulic Engineering*, *143*(8), 1–12. https://doi.org/10.1061/(asce)hy.1943-7900.0001315

USACE. (2024). *National Inventory of Dams*. https://nid.sec.usace.army.mil/#/

Wu, W. (2011). Earthen Embankment Breaching. *Journal of Hydraulic Engineering*, *137*(12), 1549–1564. https://doi.org/10.1061/(asce)hy.1943-7900.0000498

Yang;, H., Winzebrea, M. H., S. Winzenread;, & K. Okada. (1999). *The History of Dams*. University of California.

Appendix A: Tables

Table A.1: Flow Conditions

Run #	Q(m^3/s)	U(m/s)	U*	τ_b (Pa)	Yd (m)
1	0.0055	0.14	0.02	1.27	0.15
2	0.0055	0.20	0.03	2.00	0.11
3	0.0135	0.30	0.05	5.95	0.17
4	0.0180	0.37	0.06	9.3	0.19
5	0.0135	0.40	0.07	9.50	0.13
6	0.0180	0.51	0.09	11.70	0.14

Table A.2*:* Optimum Water Content of xanthan gum treated sand-silt mixtures

Silt	Water Content					
	0.05% XG	0.1% XG	0.15% XG	0.2% XG	0.3% XG	0.5% XG
0%	6%	5%	5%	7%	10%	10%
10%	12%	11%	11%	10%	10%	10%
25%	10%	8%	8%	10%	9%	10%

Table A.3: Optimum Water Content for sand-silt mixtures at 0.05% xanthan gum content

	Silt %	0%	5%	10%	15%	25%
0.05% XG	Water content	6%	10%	12%	10%	10%

Table A.4: Results of Erosion Tests

	0% Silt			10% Silt			25% Silt		
Run	0.05	0.1	0.15	0.05	0.1	0.15	0.05	0.1	0.15
1	0	0	0	0	0	0	0	0	0
2	0	0	0	0.03	0	0	0	0	0
3	0.04	0	0	0.03	0.01	0	0.01	0	0
4	0.08	0.02	0.03	0.08	0.02	0.01	0.02	0.01	0
5	0.18	0.07	0.05	0.17	0.04	0.05	0.03	0.02	0
6	0.35	0.2	0.09	0.45	0.15	0.07	0.2	0.09	0.02

Appendix B: Figures

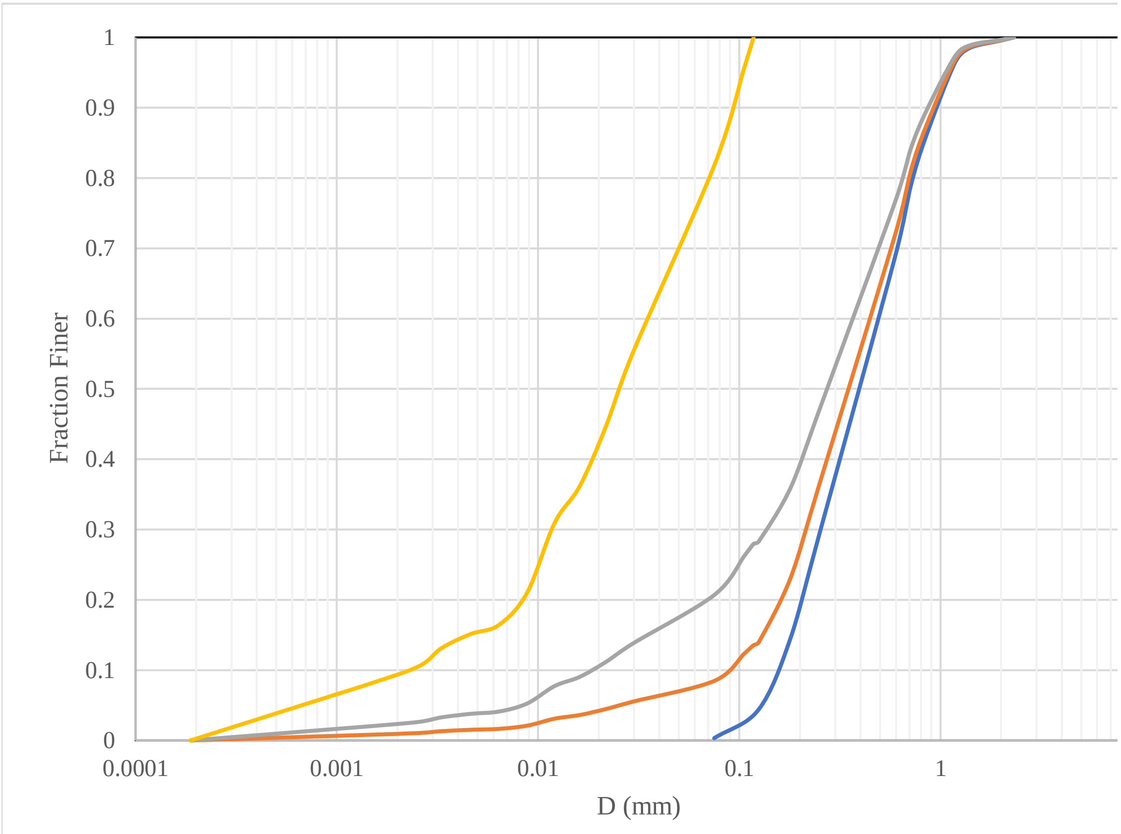

Figure B.1: Grain size distribution of sediments used in the experiments including that of silt used in creating the mixtures. The blue line indicates the grain size distribution of the sand, with geometric mean size, D_g = 0.42 mm, median diameter D_{50} = 0.44 mm and geometric standard deviation s_g = 1.81. The yellow line represents the silt grain size distribution. Two sand-silt mixtures were used in the experiments and were obtained adding 10% and 20% by mass to the sand which are the gray and orange lines shown respectively.

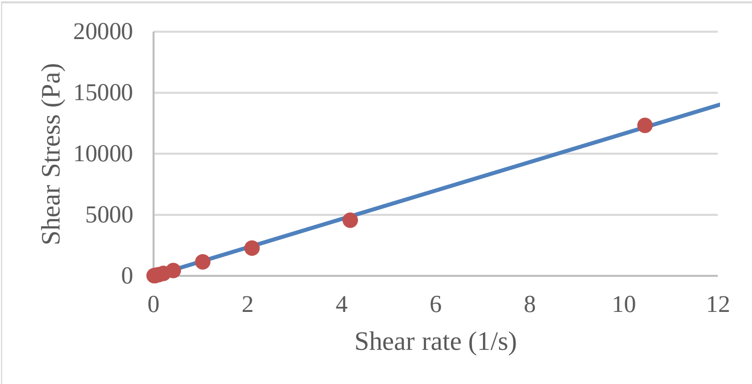

(a)

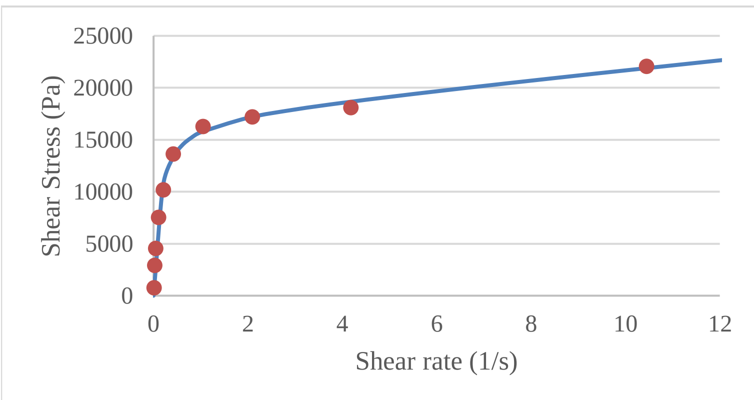

(b)

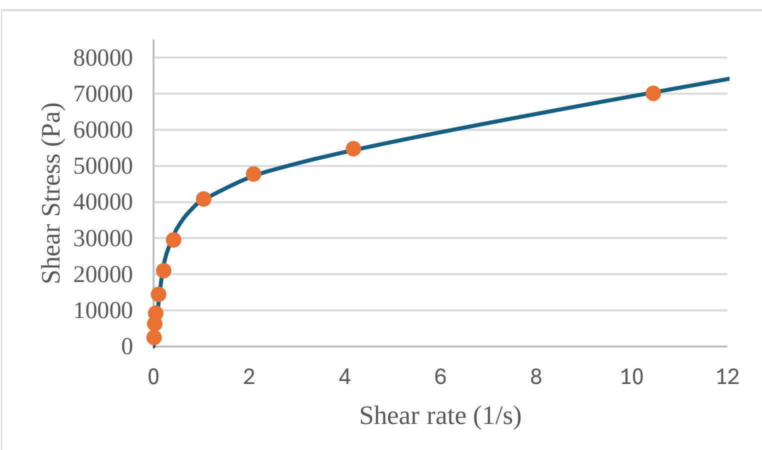

(c)

Figure B.2: Rheological model for 0.05%, 1%, and 2% (Figures 2a, b, and c respectively). Fitting parameters for τ_{ya} obtained were 23,248.68, 17,226.97, and 47,359.81 respectively. For γ_r fitting parameters were 30.03, 36.90, and 20.55 respectively. Fitting parameter for r were 0.0027, 283.99, and 83.29 respectively.

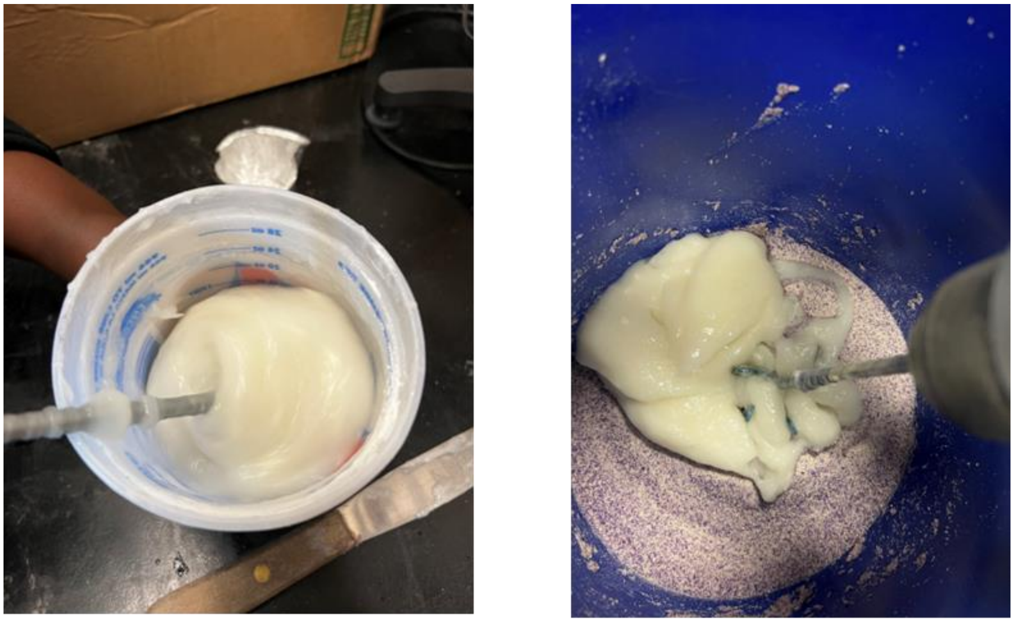

(a) (b)

Figure B.3: Mixing Of Biopolymer and Sand

Mixing xanthan gum solution with hand drill until a relatively even and viscous gel-like mixture is formed (Figure B.3a). This solution is then added to the sediment and stirred with a hand drill until the xanthan gum solution is uniformly mixed with all the sand. (Figure B.3b)

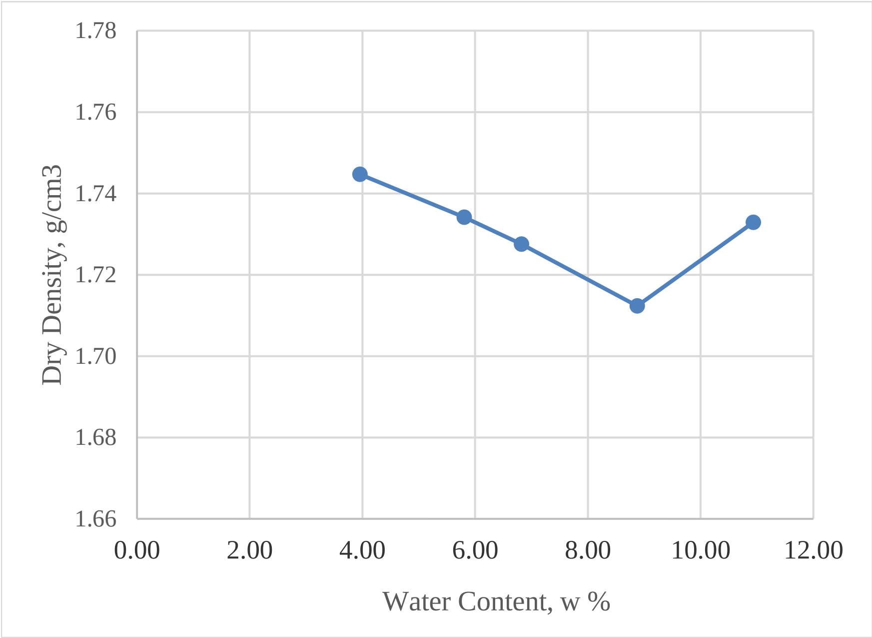

(a)

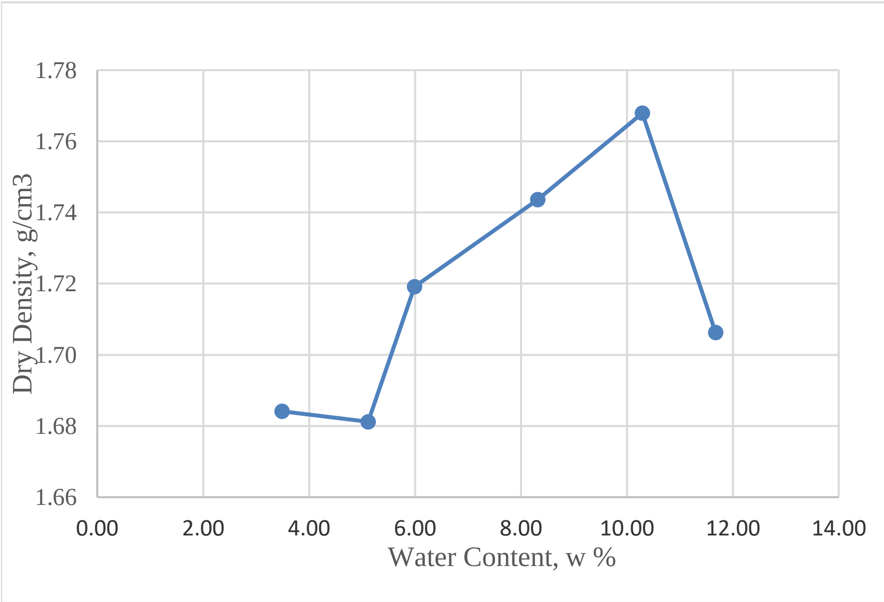

(b)

Figure B.4: Chart Showing Results for Proctor Tests For 0.5% Xanthan Gum Using the ASTM 698 (a) And USC Method (b). The optimum water content for proctor tests using ASTM 698 is determined by the maximum point following a clear rise and fall of data points. However, this is not the case looking figure a. A clear trend of rise and fall with an optimum point at the maximum can be seen with the USC method.

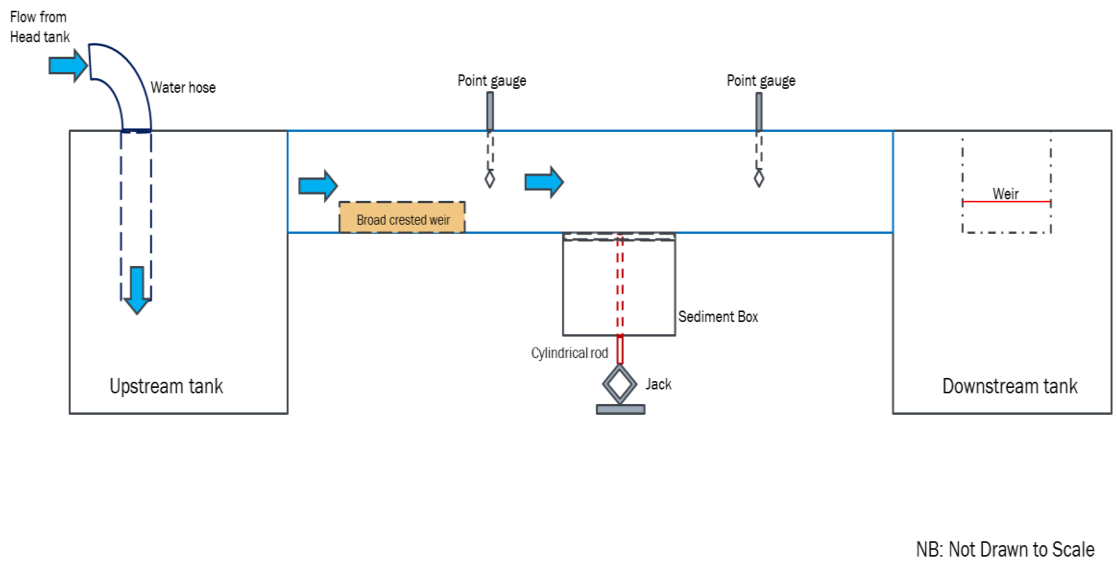

Figure B.5: Schematic of Flume Setup

A sketch of the laboratory flume used for the erodibility experiment.

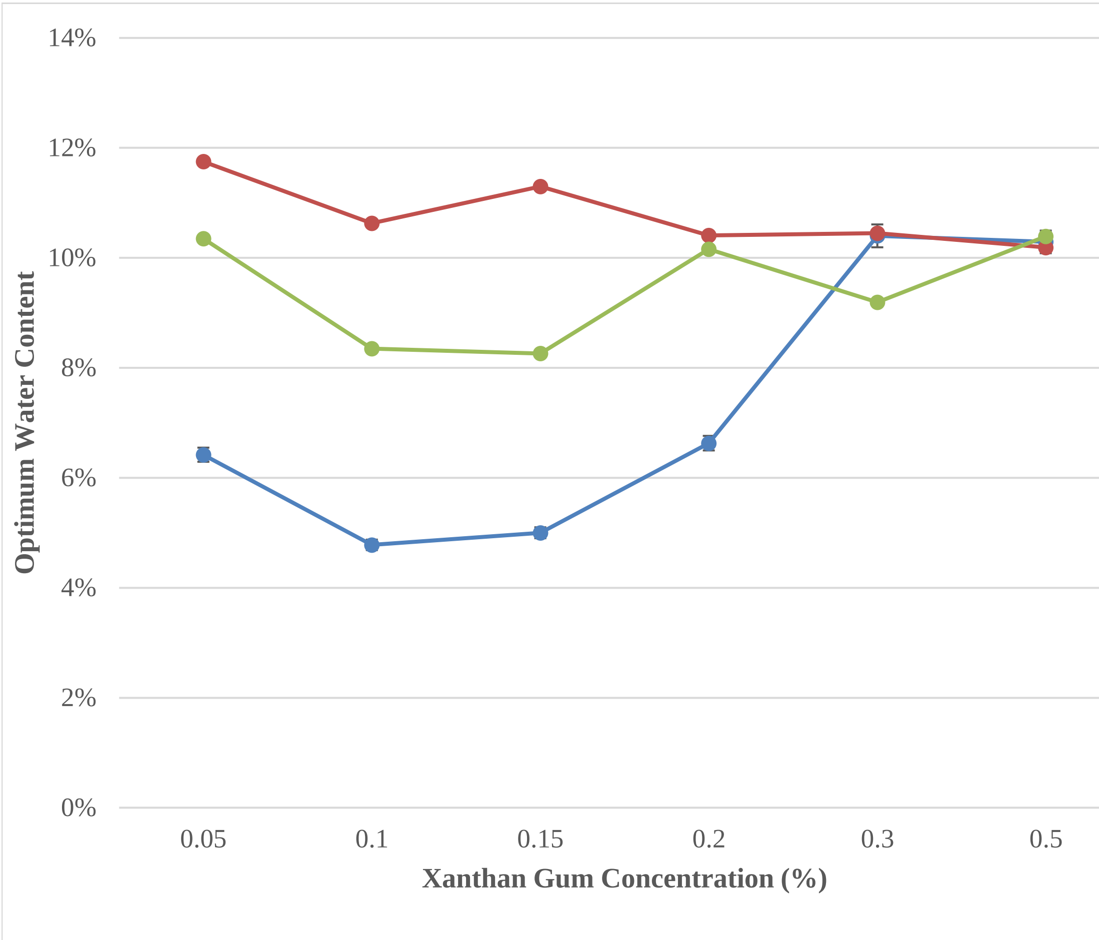

Figure B.6: Proctor Test results for different concentrations of xanthan gum and silt.

Proctor results showing that for xanthan gum concentrations smaller than 0.2%, the optimum water content increases with silt concentration until a maximum value is reached around 10% silt concentration (orange line), and then it slightly drops to the 25% silt concentration (grey line). It, however, does not seem to vary with xanthan gum concentrations greater than 0.2%.

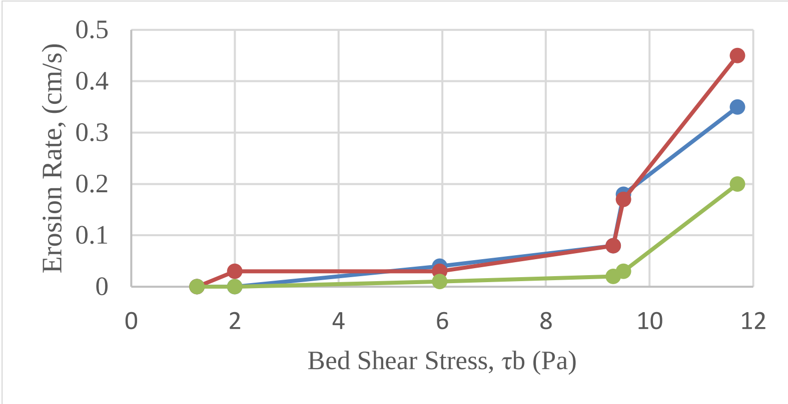

(a)

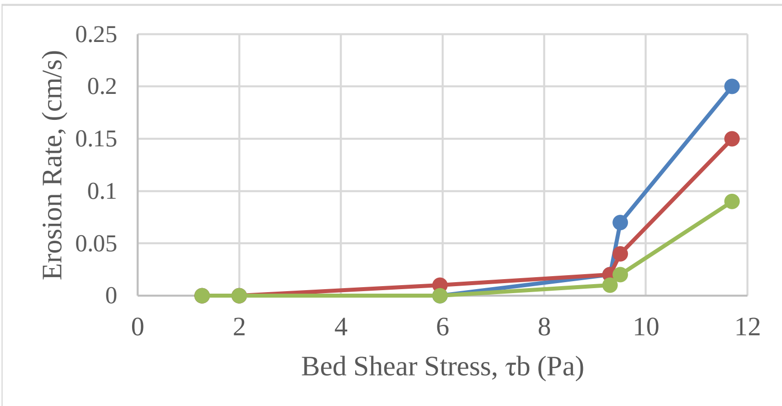

(b)

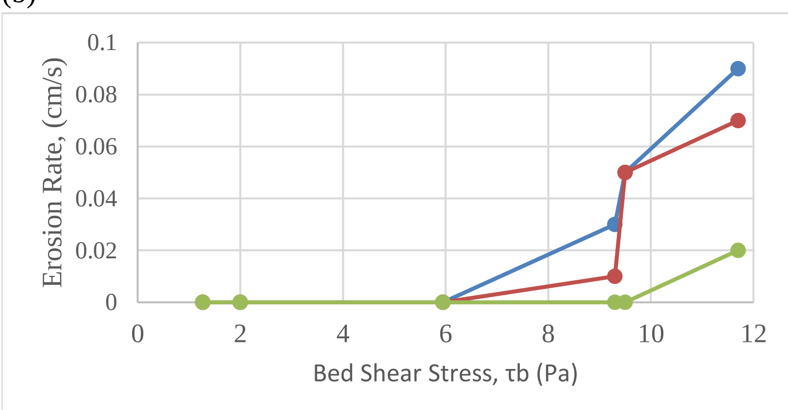

(c)

Figure B.7: Erosion rate versus bed shear stress at 0.05% xanthan gum concentration (Figure 7a), no difference is observed between the sand sample and the mixture with 10% of silt content at relatively low values of the bed shear stress. At such low xanthan gum concentration, erosion rate decreases for the mixture with 25% silt content. At higher xanthan gum concentrations (Figures 7b and 7c), erosion rate decreases with increasing silt content. In all instances, at bed shear stress greater than 9.3 Pa (runs 5 and 6), there is a sudden increase in erosion rate. This corresponds to a change in the mode of erosion, from grain-grain and abrasion to plucking. Blue, orange, and green lines indicate 0%, 10%, and 25% silt content respectively.

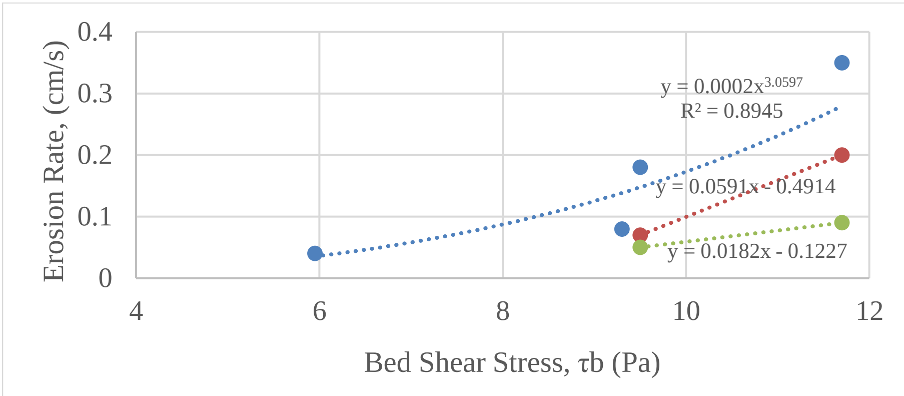

(a)

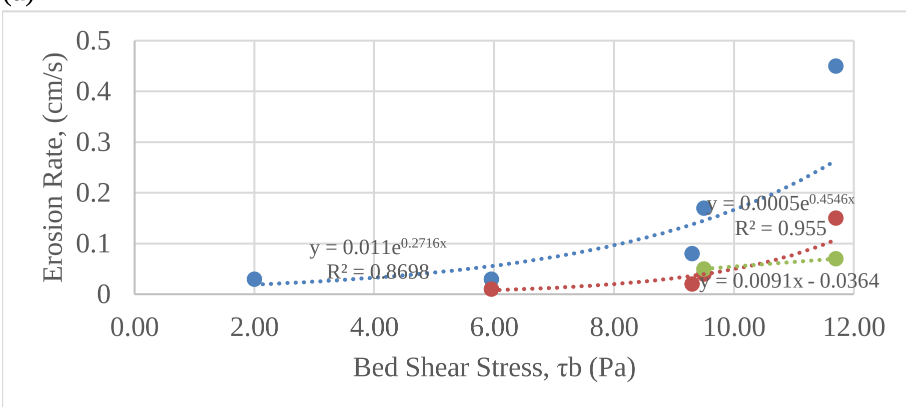

(b)

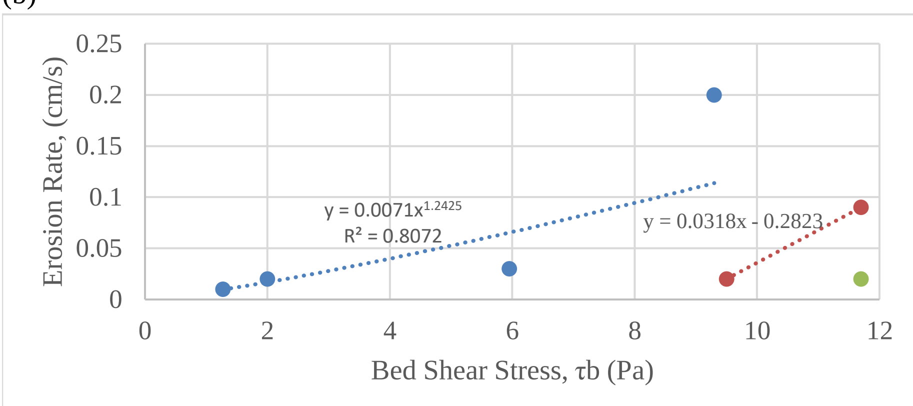

(c)

Figure B.8: Chart of Erosion Rate Vs Shear Stress. The relation between erosion rate and the bed shear stress for all the samples are shown above in Figure B.8. Chart for 0% silt (Figure B.8a) indicates a power relation between bed shear stress and erosion rate for 0.05% xanthan gum whereas 0.1% xanthan gum and 0.15% xanthan gum show a linear relationship for the range of bed shear stress that was applied. Same can be observed with 25% silt (Figure B.8c) except for 0.15% xanthan gum which was characterized by one erosion point. For 10% silt (Figure B.8b), an exponential relation provided the best fit for both 0.05% and 0.1% xanthan gum mixtures.

Appendix C: Progression Pictures of Sample

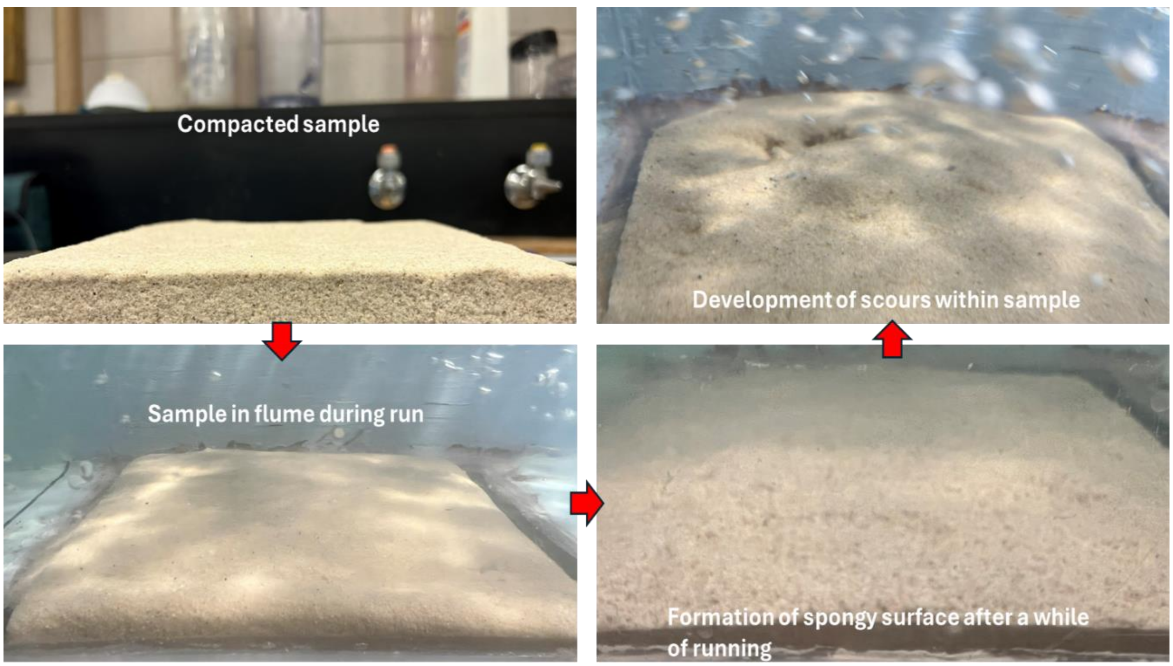

Figure C.1: The above shows how the sediment progresses through the different stages of the experiment. That is, from when it is compacted within the sediment box, to the formation of a spongy surface and lastly, the development of scours on surfaces of the sample.